# Threshold Pressure Sensing Using Parametric Resonance in Electrostatic MEMS

Md Nahid Hasan, Mark Pallay, Shahrzad Towfighian Department of Mechanical Engineering, Binghamton University

Binghamton, New York, USA Email: mhasan22@binghamton.edu, mapally1@binghamton.edu,stowfigh@binghamton.edu

Abstract— This study illustrates the concept of threshold pressure sensing using the parametric resonance of an electrostatic levitation mechanism. The electrostatic levitation allows the oscillations in the opposite direction of the substrate, thereby not limited to small gaps. The pressure sensor detects the pressure drop below a threshold value by triggering the parametric resonance with significant peak to peak dynamic amplitude changes (~ 25  $\mu m$ ). This detection relies on the fact that the instability region expands when the pressure drop forces the amplitude jump up to the higher oscillation branch. This significant change in the resonator amplitude can be related to a large capacitance variation indicating the threshold pressure. A mathematical model of the resonator is presented to show the working principle of the sensor through frequency response. Our experimental results show that the threshold pressure the sensor detects, can be adjusted by the AC voltage it receives.

# **Keywords—MEMS, Pressure Sensors, Parametric Resonance**

#### I. Introduction

Micro-electromechanical systems (MEMS) have received great attention in the last few decades with applications in the field of energy harvesting [1], Pressure sensing [2], actuation, and many others [3]. During early 1960's couple of American leading companies (Bell Labs and Honeywell research center) demonstrated the first silicon diaphragm pressure sensor [4]. The conventional design of the MEMS pressure sensor is based on the change of capacitance, resistance, or frequency shifts because of variation in displacement or stiffness of a diaphragm exposed to external pressure. Exploiting nonlinearities to improve sensing in electrostatic MEMS have been recently explored [5-7].

In this study, we have proposed a pressure sensor which is based on parametric resonance using repulsive force mechanism (fig.1) [8]. The layout of the pressure sensor consists of a cantilever beam (green) suspended above the three fixed electrodes (blue). Combined AC and DC voltage is applied to the two side electrodes that creates a net upward force on the beam. The force is in the upward direction rather than downward because the ground center electrode acts as a shield to the bottom surface of the beam causing the net electrostatic force to change the directions. As a result, the sensor is capable of eliminating

the risk of pull-in allowing much higher amplitudes caused by nonlinear effects such as parametric resonance [9]. The working principle of the threshold pressure sensor is to trigger an action when the pressure drops below a certain value. Various applications that can benefit from this capability includes switches for oxygen masks in planes, or triggers for HVAC compressors when the pressure drops below a certain value.

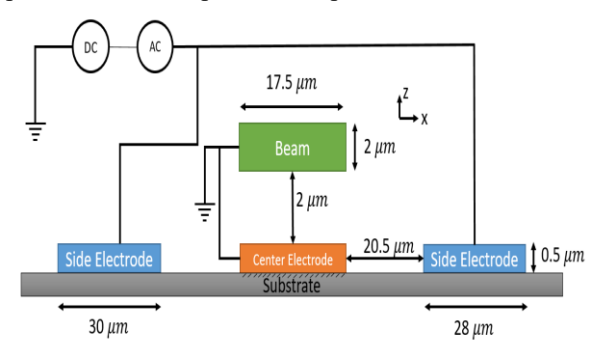


Fig.1 The layout of the pressure sensor electrodes with cantilever boundary condition.

We present the feasibility of threshold pressure sensing through simulations and measurements. The pressure drop directly changes the quality factor. Through simulation studies, we have shown how the quality factor influences the frequency response by expanding the instability region. The expansion in the instability region forces the oscillation to jump from a low to high branch when the pressure drops below a threshold. This observation qualitatively explains the blow up of the amplitude when the pressure drops that is captured by a laser vibrometer. The organization of this paper is followed respectively: model derivation, simulation results, experimental results, and conclusion.

## II. MODEL DERIVATION

Euler-Bernoulli beam theory is used to model the pressure sensor. The governing partial differential equation is given by [9],

$$\rho A \frac{\partial^2 w}{\partial t^2} + c \frac{\partial w}{\partial t} + EI \frac{\partial^4 w}{\partial x^4} + f_e(w)V^2 = 0$$
 (1)

where w is in the z-direction beam displacement, I is the moment of inertia, V is the side electrode voltage, and  $f_e$  is the electrostatic force at 1 V (side electrode voltage). The electrostatic force profile is determined with 2D COMSOL

simulation [9]. Using the parameter from Table 1, Eq. (1) is nondimensionalized, which provides equation (2). The beam has length  $L=500~\mu m$  elastic modulus E=165~Gpa, density  $\rho=2330~kg/m^3$  Poisson's ratio  $\nu=0.22$  respectively.

$$\frac{\partial^2 \widehat{w}}{\partial \widehat{t}^2} + \widehat{c}^* \frac{\partial \widehat{w}}{\partial \widehat{t}} + \frac{\partial^4 \widehat{w}}{\partial \widehat{x}^4} + r_1 V^2 \sum_{j=0}^{5} p_j h^j \widehat{w}^j = 0$$
 (2)

where  $p_j$  are the constants from the 5<sup>th</sup> order polynomial fit on the electrostatic force [9].

Table 1. Parameters for Nondimensionalization

Parameter	Substitution
<i>x</i> -direction position	$\hat{x} = x/L$
z-direction position	$\widehat{w} = w/h$
Time	$\hat{t} = t/T$
Damping	$\hat{c}^* = \frac{cL^4}{EIT}$
Time constant (s)	$T = \sqrt{\rho A L^4 / EI}$
Force constant $(m/N)$	$r_1 = L^4 / EIh$

After applying Galerkin's method, Eq. (2) gives a set of coupled ordinary differential equations (ODE). The beam response can be approximated by

$$\widehat{w}(x,t) \approx \sum_{i=1}^{n} q_i(t)\phi_i(x)$$
 (3)

where  $\widehat{w}(x,t)$  depends on a variable in space  $\phi_i(x)$  (mode shape) and a time variable  $q_i(t)$ . n is the number of degrees of freedom (DOF). The mode shapes for the cantilever are stated as

$$\phi_i(x) = \cosh(\alpha_i x) - \cos(\alpha_i x) - \sigma_i(\sinh(\alpha_i x) - \sin(\alpha_i x))$$
(4)

where  $\alpha_i$  are the square root of nondimensional natural frequencies and constant  $\sigma_i$  are obtained for the cantilever boundary conditions.

Considering the first mode approximation, Eq. (2) becomes

$$m_1\ddot{q}_1 + c_1\dot{q}_1 + k_1q_1 + r_1V^2 \sum_{i=0}^{5} f_j q_1^j = 0$$
 (5)

Where,

$$f_j = p_j h^j \int_0^1 \phi_1^{j+1} \, dx \tag{6}$$

A linear damping model is used with Eqn. (5). The damping coefficient can be estimated by the below Eq. (7) with the quality factor Q and the first natural frequency  $\alpha_1^2$ .

$$c = \frac{\alpha_1^2}{Q} \tag{7}$$

## III. SIMULATION RESULTS

Because of squeeze film effect, the spring coefficient of air will be considerable. However, to provide a qualitative explanation of the pressure sensing concept, we ignore the air spring effect and obtain the frequency response of the sensor. The numerical shooting technique is used to plot the frequency response curve to illustrate the parametric resonance. The pressure is inversely proportional to the quality factor. Decreasing the pressure (increasing the quality factor) causes a considerable peak of the displacement. Time responses, as well as steady state phase portraits of the pressure sensor, are presented for comparison. Two Quality factors Q=103 and Q=1030 have been chosen to illustrate the concept of threshold pressure sensing.

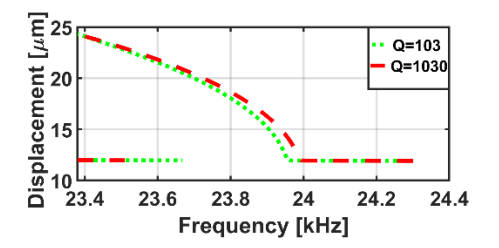


Fig.2 Frequency response at about 160  $V_{DC}$  and 16.3  $V_{AC}$ .

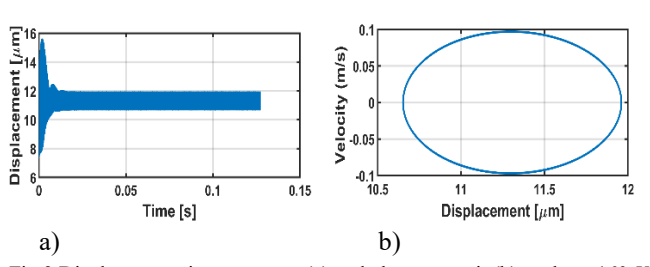


Fig.3 Displacement time response (a) and phase portrait (b) at about 160  $V_{DC}$  and 16.3  $V_{AC}$ , 23.58 kHz and Q=103 showing a considerable drop of displacement.

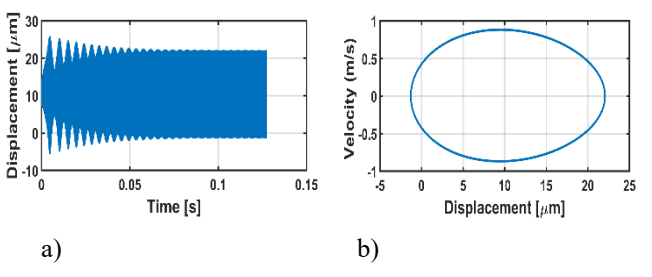


Fig.4 Displacement time response (a) and phase portrait (b) at about 160  $V_{DC}$  and 16.3  $V_{AC}$ , 23.58 kHz and Q=1030 showing parametric resonance with large amplitude.

The frequency response curve (fig.2) indicates for a frequency range, there are two stable branches (high and low). The increase in the quality factor shortens this range. That means if the operating frequency is chosen in that range and initially the response lies on the low stable branch, certain increase in the quality factor (drop of the pressure) can cause the low oscillation to become unstable. This instability pushes the beam to jump up to its higher branch oscillation. The frequency of 23.58 kHz

(twice the natural frequency ~12 kHz) is chosen as the excitation frequency to compare the time responses and phase portraits for the two different quality factors (fig. 3-4). When we drive the system at high pressure (Q=103) there is a stable oscillation near the static position (fig. 3). But if the pressure drops below to a certain threshold value (in our modeling Q = 1030) the system loses its stability in the lower branch and the system will jump up to the higher branch ( $\sim$ 25  $\mu m$ ) of the frequency response curve and shows parametric resonance (fig. 4). This blow up of amplitude causes a large change in capacitance that can be detected or can trigger an action (open/close switch) for different safety purposes. It is noted that this large amplitude is achieved despite the anchor height of  $2 \mu m$ . This travel range is possible because the large DC voltage of 160 V on the side electrodes causes the beam to travel 14  $\mu m$  above the bottom electrode that enables the peak to peak dynamic amplitude as high as  $28 \mu m$ .

## IV. EXPERIMENTAL RESULTS

Fig. 5 shows the schematic diagram of the experimental setup. MSA-500 laser vibrometer was used for the dynamic measurement. MATLAB data acquisition toolbox and a National Instrument USB 6366 Data acquisition tool were used for signal processing and acquiring data from the vibrometer. Krohn-Hite 7600 Wideband Power Amplifier is used to apply superimposed DC offset voltage and for the amplification of the AC voltage. The fabrication of the resonator was done by MEMSCAP [10].

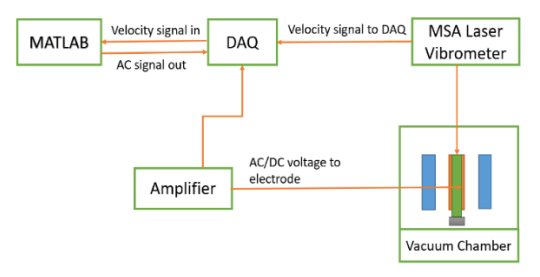


Fig.5 Experimental setup of the MEMS pressure sensor.

To demonstrate the tunability of the threshold pressure, at a fixed excitation frequency 23.58 kHz and at the fixed  $V_{DC}$ =160V, we have varied the pressure and the AC voltage to find the threshold pressure where parametric resonance is triggered (fig. 6a). The figure shows how the sensor can be set to detect drop of pressure below a certain pressure value. For example, if the pressure of interest is 400 Pa, the AC voltage of the sensor should be set to 24 V to activate the parametric resonance at pressures equal to or below 400 Pa. Qualitative validation of activation of parametric resonance can be observed in experiments (fig. 6b) and simulations (fig. 4a). When AC= 16.3 V, in the experiments, the pressure drop below 133.322 Pa causes the blow up in the amplitude, while the simulation shows the quality factor in excess of 1030 leads to the sudden amplitude increase. Both of these observations indicate the expansion of instability region when the pressure drops that is used to illustrate the threshold pressure sensing concept. In order to obtain a quantitative agreement between the experiments and simulations, more in depth analysis must be done on the fluidsolid interactions that can cover small as well as large oscillation ranges.

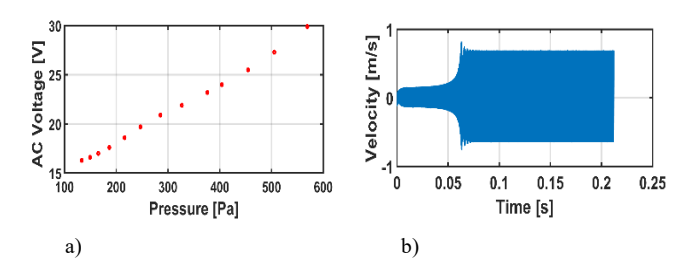


Fig.6 (a) AC voltage vs pressure curve from activation of parametric resonance (b) beam tip velocity time series measured by a laser vibrometer showing parametric resonance at 133.322 Pa pressure and 160  $V_{DC}$  and 16.3  $V_{AC}$ .

#### V. CONCLUSION

In conclusion, we illustrated the concept of pressure sensing based on parametric resonance for an electrostatic levitation MEMS device. The electrostatic levitation mechanism enables large oscillations without the danger of pull-in and hitting the lower electrode. The parametric resonance with significant oscillation amplitude is activated at twice the natural frequency when the pressure drops below a threshold. This large amplitude oscillation can create a jump in the capacitance and its detection can create alarm or trigger an action. The threshold pressure is tuned by varying the AC voltage of the sensor to offer a versatile pressure sensor for different applications.

# VI. ACKNOWLEDGEEMNT

Financial support of this study was provided by NSF ECCS grant # 1608692.

#### REFERENCES

- [1] K. A. Cook-Chennault, N. Thambi, and A. M. Sastry, "Powering MEMS portable devices A review of non-regenerative and regenerative power supply systems with special emphasis on piezoelectric energy harvesting systems," *Smart Mater. Struct.*, vol. 17, no. 4, 2008.
- [2] P. K. Kinnell and R. Craddock, "Advances in Silicon Resonant Pressure Transducers," *Procedia Chem.*, vol. 1, no. 1, pp. 104–107, 2009
- [3] P. K. Pattnaik, B. Vijayaaditya, T. Srinivas, and A. Selvarajan, "Optical MEMS pressure sensor using ring resonator on a circular diaphragm," *Proc. - 2005 Int. Conf. MEMS, NANO Smart Syst.* ICMENS 2005, pp. 277–280, 2005.
- [4] H. Hejun and R. Bogue, "MEMS sensors: Past, present and future," Sens. Rev., vol. 27, no. 1, pp. 7–13, 2007.
- [5] W. M. Zhang, H. Yan, Z. K. Peng, and G. Meng, "Electrostatic pullin instability in MEMS/NEMS: A review," Sensors Actuators, A Phys., vol. 214, pp. 187–218, 2014.
- [6] A. H. Nayfeh and M. I. Younis, "Dynamics of MEMS resonators under superharmonic and subharmonic excitations," J. Micromechanics Microengineering, 2005.
- [7] K. L. Turner, S. A. Miller, P. G. Hartwell, N. C. Macdonald, and S. H. Strogatz, "Five parametric resonances in a mems.pdf," vol. 396, no. November, pp. 149–152, 1998.
- [8] M. Pallay, M. Daeichin, and S. Towfighian, "Dynamic behavior of an electrostatic MEMS resonator with repulsive actuation," *Nonlinear Dyn.*, vol. 89, no. 2, pp. 1525–1538, 2017.
- [9] M. Pallay and S. Towfighian, "A parametric electrostatic resonator

using repulsive force," *Sensors Actuators, A Phys.*, vol. 277, pp. 134–141, 2018.

A. Cowen, B. Hardy, R. Mahadevan, and S. Wilcenski, "PolyMUMPs Design Handbook." [10]